

# The Enabling Electronic Motif for Topological Insulation in $ABO_3$ Perovskites

Xiuwen Zhang,<sup>\*</sup> Leonardo B. Abdalla, Qihang Liu,<sup>\*</sup> and Alex Zunger<sup>\*</sup>

Stable oxide topological insulators (TIs) have been sought for years, but none have been found; whereas heavier (selenides, tellurides) chalcogenides can be TIs. The basic contradiction between topological insulation and thermodynamic stability is pointed out, offering a narrow window of opportunity. The electronic motif is first identified and can achieve topological band inversion in  $ABO_3$  as a lone-pair, electron-rich B atom (e.g., Te, I, Bi) at the octahedral site. Then, twelve  $ABO_3$  compounds are designed in the assumed cubic perovskite structure, which satisfy this electronic motif and are indeed found by density function theory calculations to be TIs. Next, it is illustrated that poorly screened ionic oxides with large inversion energies undergo energy-lowering atomic distortions that destabilize the cubic TI phase and remove band inversion. The coexistence windows of topological band inversion and structure stability can nevertheless be expanded under moderate pressures (15 and 35 GPa, respectively, for  $BaTeO_3$  and  $RbIO_3$ ). This study traces the principles needed to design stable oxide topological insulators at ambient pressures as a) a search for oxides with small inversion energies; b) design of large inversion-energy oxide TIs that can be stabilized by pressure; and c) a search for covalent oxides where TI-removing atomic displacements can be effectively screened out.

such heavy-atom compounds tend to pose defective crystal structures (e.g., spontaneous vacancy formation causing metallic behavior) associated with the relatively low cohesion of the weak heavy-atom chemical bonds.<sup>[12–14]</sup> The recent quest of topological insulators in oxides<sup>[15–21]</sup> has been partially motivated by the hope that this will deliver defect-tolerant lattices, often characteristic of metal oxides,<sup>[22]</sup> while at the same time affording the integration of topological properties with rich oxide functionalities, such as transparent conductivity,<sup>[23]</sup> ferroelectricity,<sup>[24]</sup> ferromagnetism,<sup>[25]</sup> or superconductivity.<sup>[26]</sup> However, the electronic structures of common octet metal oxides, such as  $ABO_3$  perovskites or  $A_2BO_4$  spinels, show that, while they may be stable and have wide energy band gaps

f. . . g, . . . , . . . , f. . . g  
g  
f  
Q30,  
g  
g  
f. . . g  
g f  
g  
g 51 Q60, . . .

DOI: 10.1002/adfm.201701266

origin of the hitherto mysterious difficulty to obtain simultaneously electronic band inversion and thermodynamic stability. We will refer to the electronic structure associated with the geometrical motif shown in Figure 1 (which we will show, enables topological insulation) as the “topological gene.” We then identify the topological gene in oxide perovskites as being a lone-pair electron-rich B atom (e.g., Te, I, Bi rather than Ti, Nb, Y, respectively) at the octahedral site in the cubic  $ABO_3$ . Oxides tend to have larger predicted inversion energies ( $\Delta$

There are also some 2D oxides that have been predicted theoretically to be TIs in hypothetical structures.<sup>[19–21]</sup> Examples include the assumed (111) bilayers of LaAuO<sub>3</sub> and SrIrO<sub>3</sub> compounds, which, however, were shown to undergo TI to antiferromagnetic insulator transition.<sup>[20]</sup> Similarly, a single monolayer of ZrSiO, assumed to be exfoliated from its stable 3D layered form, has recently been predicted to be a topological insulator.<sup>[21]</sup> However, given the large calculated binding energy >1 eV of the 2D ZrSiO monolayer to its bulk 3D lattice,<sup>[21]</sup> one would doubt if the isolated 2D layer could be stabilized. Another topological property (Dirac semimetal) was theoretically illustrated<sup>[29]</sup> in BiO<sub>2</sub> in the assumed  $\beta$ -cristobalite (SiO<sub>2</sub>) structure (forcing a 4+ oxidation state on Bi); however, its stable experimental structure<sup>[30]</sup> ( $\beta$ -Sb<sub>2</sub>O<sub>4</sub>-type, C2/c, a charge ordered structure with stable oxidation states 3+ and 5+ of Bi) that has much lower total energy than  $\beta$ -cristobalite BiO<sub>2</sub>,<sup>[31,32]</sup> is a normal insulator.

### 3. Topological Gene and Stability Gene

To address the issue of possible conflict between band inversion and stability, we introduce two constructs: We first identify

an electronic motif within a group of ABO<sub>3</sub> oxides that would generate band inversion—the “topological gene” of this group of compounds. As Figure 1c,d illustrates, the topological gene here is the octahedral BO<sub>6</sub> motif with lone-pair B atom (generated, e.g., by replacing an electron-poor Ti atom in BaTiO<sub>3</sub> by an electron-rich Te atom in BaTeO<sub>3</sub> that has an additional d<sup>10</sup>s<sup>2</sup> shell). Second, we examine the stability of the crystal structure that hosts the topological gene, relative to the ground state structures that hosts the “stability gene” of this group of compounds. The key challenge is to see if structures with the topological gene can also have the stability gene. Thus, coevaluation of the electronic structure and stability is required.<sup>[37]</sup>



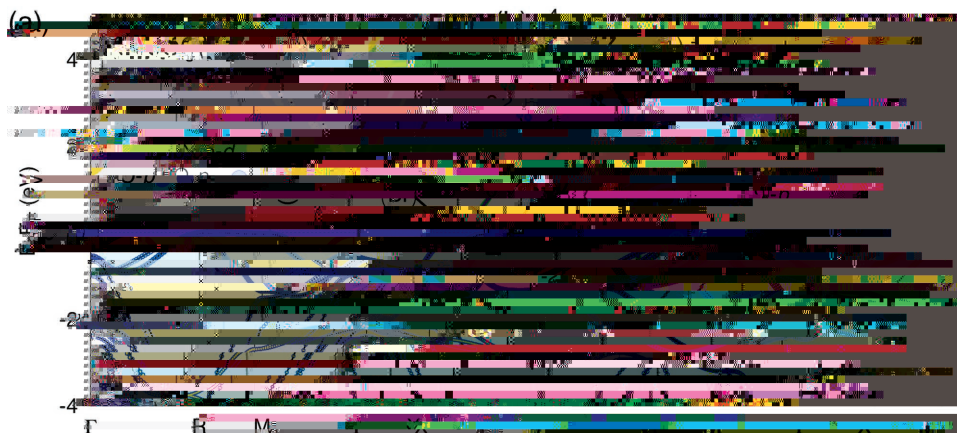


Figure 3. Band structure plot showing energy (eV) versus momentum along the high-symmetry path  $\Gamma$ -R-M<sub>2</sub>- $\Gamma$ . The plot displays multiple bands with a clear band gap around 0 eV.

being the lowest-energy structures of specific ABO<sub>3</sub> compounds, relative to the lowest-energy phase. The A position in ABO<sub>3</sub> with the S1 (prototype compound: CaTiO<sub>3</sub>) structure is the cube vertices (Ca sites in CaTiO<sub>3</sub>) and the B position is part of the BO<sub>6</sub> octahedra (Ti sites in TiO<sub>6</sub> of CaTiO<sub>3</sub>), similarly for S2–S15 types. We considered the swapping of A and B elements on the ABO<sub>3</sub> atomic site to create BAO<sub>3</sub>, and found that this lowers the energy for 33 structures in our calculations, which are marked by italic text in Figure 4, meaning that the lowest energy structure is BAO<sub>3</sub>. The lattice parameters (as well as band gaps) of the relaxed crystal structures

in Figure 4 are provided in Table S1 (Supporting Information). In addition to stability, Figure 4 also denotes if according to the calculated topological invariant  $Z_2$  the compound is a TI or a normal insulator. We find from such total energy minimizations that the BO<sub>6</sub> octahedral unit with the said electron rich B atom tends to distort toward a stabler, noncubic crystal structure<sup>[31,32]</sup> and that this distortion removes the topological insulation. Therefore, the stability gene and TI gene tend to contradict each other for the ABO<sub>3</sub> compounds at ambient conditions: ABO<sub>3</sub> oxides that are stable are not TIs and structures that are TIs are not stable.

II <sub>A</sub>	Te	Se	II <sub>B</sub>	Ti	Bv	Ga/In/Pa	Al/Sb/As
Ba	BaTeO <sub>3</sub>	BaSeO <sub>3</sub>	BaTiO <sub>3</sub>	BaVO <sub>3</sub>	BaBiO <sub>3</sub>	BaGaO <sub>3</sub>	BaAlO <sub>3</sub>
	<i>S1 (26): NI</i>	<i>S1 (26): NI</i>	<i>S1 (26): NI</i>	<i>S1 (26): NI</i>	<i>S1 (26): NI</i>	<i>S1 (26): NI</i>	<i>S1 (26): NI</i>
	S2 (76): NI	S3 (37): NI	S3 (37): NI	S3 (37): NI	S3 (37): NI	S3 (37): NI	S3 (37): NI
	S4 (15): NI	S4 (15): NI	S4 (15): NI	S4 (15): NI	S4 (15): NI	S4 (15): NI	S4 (15): NI
Sr	SrTeO <sub>3</sub>	SrSeO <sub>3</sub>	SrTiO <sub>3</sub>	SrVO <sub>3</sub>	SrBiO <sub>3</sub>	SrGaO <sub>3</sub>	SrAlO <sub>3</sub>
	<i>S1 (232): NI</i>	<i>S1 (232): NI</i>	<i>S1 (232): NI</i>	<i>S1 (232): NI</i>	<i>S1 (232): NI</i>	<i>S1 (232): NI</i>	<i>S1 (232): NI</i>
	S2 (43): NI	S2 (43): NI	S2 (43): NI	S2 (43): NI	S2 (43): NI	S2 (43): NI	S2 (43): NI
	S4 (52): NI	S4 (52): NI	S4 (52): NI	S4 (52): NI	S4 (52): NI	S4 (52): NI	S4 (52): NI
Ca	CaTeO <sub>3</sub>	CaSeO <sub>3</sub>	CaTiO <sub>3</sub>	CaVO <sub>3</sub>	CaBiO <sub>3</sub>	CaGaO <sub>3</sub>	CaAlO <sub>3</sub>
	<i>S1 (47): NI</i>	<i>S1 (47): NI</i>	<i>S1 (47): NI</i>	<i>S1 (47): NI</i>	<i>S1 (47): NI</i>	<i>S1 (47): NI</i>	<i>S1 (47): NI</i>
	S2 (52): NI	S2 (52): NI	S2 (52): NI	S2 (52): NI	S2 (52): NI	S2 (52): NI	S2 (52): NI
	S3 (17): NI	S3 (17): NI	S3 (17): NI	S3 (17): NI	S3 (17): NI	S3 (17): NI	S3 (17): NI

Figure 4. Table showing the lowest-energy structures of specific ABO<sub>3</sub> compounds, relative to the lowest-energy phase. The table lists the structure type (S1-S15), the compound name, and the topological invariant  $Z_2$  (NI for normal insulator, TI for topological insulator). Structures marked with italics indicate that the lowest energy structure is BAO<sub>3</sub>.

## 6. Model DFT Calculation of the Evolution of the Electronic Structures with Decreasing Inversion Energy

To get a deeper understanding on the interplay between structural stability and band inversion, we perform constrained DFT calculations constructed for tuning band inversion to examine its effect on the total energy. The tuning of the inversion energy can be done by using an external potential that shifts upward the B atom  $p$  orbital energy, thus, according to Figure 1d, the inverted structure ( $p$ -below- $s$ ) can be tuned to be uninverted ( $s$ -below- $p$ ). This constraint can be implemented, for example, by adding an external potential term<sup>[45]</sup>  $V_p$  to the DFT Hamiltonian acting on the  $I-p$  orbital in  $\text{RbIO}_3$ . We then monitor the total energy of the cubic perovskite structure (S1) relative to its stable R3m rhombohedral phase (S2 in Table 1) as a function of  $\Delta_i$ . Figure 5a shows that as  $\Delta_i$  decreases, the energy of the cubic S1 phase (relative to S2) also decreases, indicating that band inversion is contraindicated with the stability of crystal structure.

Figure 6 illustrates the evolution of band structures of cubic  $\text{RbIO}_3$  with inversion energies tuned by  $V_p$ , demonstrating that as the inversion energy decreases ( $V_p$  increases), the  $I-p$  states moves up relative to the  $I-s$  states and the  $p$ -below- $s$  band inversion is gradually removed. The method of adding to the Hamiltonian an external potential  $V_p$  to independently control the band inversion is a useful device for answering the question of whether the band inversion energetically drives the structural distortions, or whether other factors drive the structural distortions and the band inversion is removed only as a side effect (it is the former). However, we remind the reader that this potential term does not represent an actual material. Figure 6c shows the band structure of cubic  $\text{RbIO}_3$

demonstrate that the cubic perovskite (S1, see red squares in Figure 7a,b) tends to be stabilized by external pressure. At pressure of 15 GPa (35 GPa), the S1 phase that contains the topological gene becomes the lowest-enthalpy structure for  $\text{BaTeO}_3$  ( $\text{RbIO}_3$ ). We further check the effect of external pressure on the band inversions in cubic  $\text{BaTeO}_3$  and  $\text{RbIO}_3$ , finding that the band inversion is not removed by external pressure (see Figure 7c,d), but on the contrary, increased by the pressure from 2.3 eV at 0 GPa to 3.4 eV at 35 GPa for  $\text{BaTeO}_3$ , and from 3.0 eV at 0 GPa to 3.8 eV at 35 GPa for  $\text{RbIO}_3$ .

unstable than band-inverted oxides is because destabilizing band inversion drives structural distortions that often remove the topo-





- 1 . . . . . g . . . . . , *Nat. Commun.* **2011**, *2*, 5 6.
- 20 . . . . . , *Phys. Rev. B* **2014**, *89*, 1 5121.
- 21 . . . . . g, . . . . . g, . . . . . g, . . . . . , *Phys. Rev. B* **2015**, *92*, 205310.
- 22 . . . . . , *Metal Oxides: Chemistry and Applications*, . . . . . , **2006**.
- 23 . . . . . , *Nature* **1997**, *389*, 3 .
- 24 . . . . . , *Nature* **1992**, *358*, 136.
- 25 . . . . . , *Handbook of Modern Ferromagnetic Materials*, . . . . . g , **1999**.
- 26 . . . . . , *Z. Phys. B: Condens. Matter* **1986**, *64*, 1 4.
- 27 *Inorganic Crystal Structure Database*, . . . . . f , . . . . . , **2006**.
- 28 . . . . . , *Inorg. Chem.* **2013**, *52*, 547 .
- 2 . . . . . g, . . . . . , . . . . . , . . . . . , . . . . . , *Phys. Rev. Lett.* **2012**, *108*, 140405.
- 30 . . . . . , . . . . . , . . . . . g , *J. Solid State Chem.* **1995**, *116*, 2 4.
- 31 . . . . . , . . . . . , . . . . . g, . . . . . , . . . . . , . . . . . , *J. Comput. Mater.* **2015**, *1*, 15010.
- 32 . . . . . g, . . . . . , . . . . . , . . . . . , . . . . . , *APL Mater.* **2013**, *1*, 011002.
- 33 . . . . . , . . . . . , *J. Cryst. Growth* **1989**, *94*, 567.
- 34 . . . . . g, . . . . . g , *Phys. Rev. Lett.* **2003**, *90*, 256401.
- 35 . . . . . , . . . . . g , *Phys. Rev. B* **1989**, *40*, 4062.
- 36 . . . . . g , . . . . . g , *Nature* **2008**, *453*, 763.
- 37 . . . . . g, . . . . . , . . . . . g , *Adv. Func. Mater.* **2016**, *26*, 325 .
- 38 . . . . . , . . . . . , . . . . . f, *Phys. Rev. Lett.* **1996**, *77*, 3 45.
- 39 . . . . . , . . . . . , *Comput. Mater. Sci.* **1996**, *6*, 15.
- 40 . . . . . , . . . . . , *Phys. Rev. B* **1999**, *59*, 175 4.
- 41 . . . . . , . . . . . , . . . . . g, . . . . . g, . . . . . , *Phys. Rev. B* **2011**, *84*, 07511 .
- 42 . . . . . , *Phys. Rev. B* **2007**, *76*, 045302.
- 43 . . . . . , . . . . . , . . . . . f, *J. Chem. Phys.* **2003**, *118*, 207 .
- 44 . . . . . , *Proc. R. Soc. A* **1928**, *118*, 654.
- 45 . . . . . , . . . . .